Design trade-offs for silicon-on-insulator-based AWGs for (de)multiplexer applications

Shibnath Pathak,* Dries Van Thourhout, and Wim Bogaerts

Photonics Research Group (INTEC), Ghent University—imec, Sint-Pietersnieuwstraat 41, B-9000 Ghent, Belgium
**Corresponding author: Shibnath.Pathak@intec.UGent.be*

Received June 17, 2013; revised July 11, 2013; accepted July 11, 2013;
posted July 11, 2013 (Doc. ID 192277); published August 5, 2013

We demonstrate compact silicon-on-insulator-based arrayed waveguide gratings (AWGs) for (de)multiplexing applications with a large free spectral range (FSR). The large FSR is obtained by reducing the arm aperture pitch without changing the device footprint. We demonstrate 4×100 GHz, 8×250 GHz, and 12×400 GHz AWGs with FSRs of 6.9, 24.8, and 69.8, respectively. We measured an insertion loss from −2.45 dB for high to −0.53 dB for low-resolution AWGs. The crosstalk varies between 17.12 and 21.37 dB. The bandwidth remains nearly constant, and the nonuniformity between the center wavelength channel and the outer wavelength channel improves with larger FSR values.

OCIS codes: (130.0130) Integrated optics; (130.1750) Components; (130.7408) Wavelength filtering devices; (130.3120) Integrated optics devices.
http://dx.doi.org/10.1364/OL.38.002961

Arrayed waveguide gratings (AWGs) are commonly used components in wavelength division multiplexing (WDM) systems for wavelength (de)multiplexing [1] and routing applications [2]. AWGs are realized in different material platforms and cover various wavelength ranges. Different platforms impose different design restrictions and opportunities for both star couplers and array waveguides. Compared to low-contrast material platforms such as silica-on-silicon and InP [3,4], high-contrast silicon-on-insulator (SOI) waveguides allow much sharper bends, reducing the device size by several orders of magnitude. But the high-contrast waveguides also have a higher propagation loss and are highly sensitive to phase errors. As a result, demonstrated silicon AWGs [5–7] exhibit a relatively high insertion loss and crosstalk, especially in devices with higher resolution, which require longer and more delay lines in the waveguide array. Therefore, in SOI it is difficult to design AWG demultiplexers with small channel spacing and large free spectral range (FSR).

In this Letter we propose an improved design procedure that leads to an optimized performance for such devices. We illustrate this procedure through the design and characterization of three sets of SOI AWGs with 100, 250, and 400 GHz channel spacing, respectively. The devices are analyzed in terms of insertion loss, crosstalk, bandwidth, and nonuniformity between the center and outer channels. Clear trends toward optimized designs are observed.

The constant length difference (ΔL) between two successive waveguides in the array section of an AWG sets its FSR as $\Delta\lambda_{\mathrm{FSR}} = \lambda_c^2/(n_{\mathrm{group}}\Delta L)$, where n_{group} is the group index of the waveguide, λ_c is the center wavelength, and $\Delta\lambda_{\mathrm{FSR}}$ is the FSR. The dispersion $D = \Delta s/\Delta\lambda$ of the waveguide array, defined as the displacement of the focal spot along the image plane per unit of wavelength change, is given by

$$D = R_a \frac{\Delta\theta_a}{\Delta\lambda}, \tag{1}$$

$$= \frac{R_a}{\Delta\lambda} a \sin\left[\left(\frac{\lambda_c}{d_a \Delta\lambda_{\mathrm{FSR}}}\right)\left(\frac{\lambda_c n_{\mathrm{eff}}(\lambda) - \lambda n_{\mathrm{eff}}(\lambda_c)}{n_{\mathrm{group}} n_{\mathrm{slab}}(\lambda_c)}\right)\right], \tag{2}$$

where $n_{\mathrm{slab}}(\lambda_c)$ is the effective index of the waveguide mode in the slab regions at the center wavelength λ_c, R_a is the focal length of the free propagation region [shown in Fig. 1(d)], θ_a is the diffraction angle, and d_a is the arm aperture pitch. As shown in Fig. 1(d), d_a is determined by the sum of the aperture waveguide width and the gap between two neighboring waveguides (with this gap chosen as the minimum spacing allowed by the technology platform, typically 100 nm in our case). If we keep the channel spacing and the dispersion fixed, increasing the FSR requires either increasing the focal length (R_a) or decreasing the arm aperture pitch d_a. The first option, increasing R_a, results in a significantly increased device size and associated with that a larger propagation loss, a stronger defocusing effect [8], and increased phase errors, all undesirable. On the other hand, if we increase the FSR by decreasing d_a, the total device size remains the same: given that the total acceptance angle θ_{acc} of the array remains the same, this option does mean we have to increase the number of waveguides ($\theta_{\mathrm{acc}} = N \times d_a$), but as the FSR scales inversely proportional to ΔL the maximum waveguide length remains the same. As an example, Figs. 1(a) and 1(f) show two 8×250 GHz AWGs with arm aperture widths of 2.75 and 1.65 μm, respectively, and 25 and 40 waveguides, respectively, in the array. The total footprint remains unchanged between both devices, but the FSR has increased from 16.8 to 26.6 nm by decreasing the aperture width.

Decreasing the arm aperture pitch has a significant impact on the performance of the AWG. The propagation loss and the imaging quality of the array are the main factors contributing to the insertion loss of the device. Given that the average length of the delay lines remains unchanged, the total propagation loss will not increase.

Furthermore, for a fixed number of channels, the increasing FSR will decrease the rolloff of the transfer characteristic for the outer channels, resulting in a

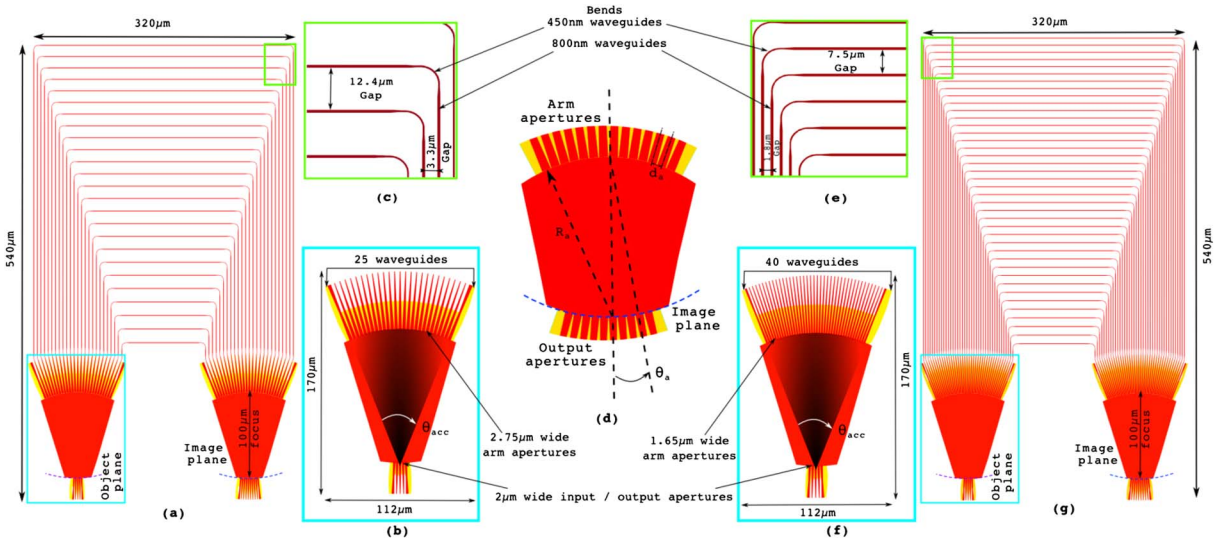

Fig. 1. Design details of 8 × 250 GHz AWGs. (a) Device with 25 waveguides in the array. (g) Device with 40 waveguides in the array. (b) and (f) Input star coupler of the device in (a) and (g), respectively. (c) and (e) Zoom into waveguide array regions for the device in (a) and (g), respectively. (d) Detailed overview of the star coupler.

smaller nonunformity between the inner and outer channels. This can be explained by the fact that the spectral response of the AWG follows the envelope of the far field of a single arm aperture. A narrower arm aperture has a wider far field, resulting in a slower rolloff for positions near the center. The bandwidth of the individual wavelength channels, on the other hand, will remain constant as the channel spacing, the dispersion in the object plane (D), and the width of the input and output apertures are kept fixed with the variation of the arm aperture pitch and the FSR. This also implies that the neighboring channel crosstalk will remain unchanged for the larger FSR devices. Also the effect on the crosstalk floor due to phase error in the waveguide array will be small as the average length of the waveguide remains unaltered.

The main limitation to further increasing the number of waveguides and the FSR is the decreasing spacing between the waveguides in the array itself as shown in Figs. 1(c) and 1(d). The reduced distance can introduce coupling between the waveguides, possibly resulting in additional phase errors. Another limitation is that we cannot reduce the arm aperture width below its critical width, for which the mode is no longer confined in the core of the waveguide and the propagation loss increases significantly.

All the AWGs were fabricated on 200 mm SOI wafers with a 220 nm thick silicon guiding layer on top of a 2 μm buried oxide layer. To pattern the designs we used 193 nm deep UV lithography and a double etch process: 220 nm deep trenches define the high-contrast waveguides (further referred to as the deep etch) as well as the sharp bends and 70 nm etch defined fiber grating couplers and lower-contrast apertures in the star coupler regions (further referred to as shallow etch). See [9] for further fabrication details.

We designed three sets of AWGs for three different channel spacings. Each of these three sets (4 × 100 GHz, 8 × 250 GHz, and 12 × 400 GHz) of AWGs has four variations of the number of waveguides used in the array waveguides, thereby also varying the FSR (see third paragraph). See [5,6] for design details of the SOI AWGs. The focal length of the star couplers was kept constant for each of those sets of AWG designs at 80, 100, and 120 μm, respectively. Table 1 gives further design details for each of the fabricated devices.

To characterize the AWGs, the input and output channels are connected to 1D grating couplers (as shown in Fig. 2). The coupling efficiency [10] with standard single-mode fiber is nearly 30%. In the measurements reported here we normalized the transmission spectrum of the AWGs with respect to that of a straight waveguide with the same type of grating couplers. The optical fibers were aligned to the grating couplers on an automated alignment setup, which uses a reproducible and wavelength-corrected algorithm to align with an accuracy of 0.01 μm in the X, Y, Z directions. Figure 2 shows optical microscope images of the fabricated AWGs.

Figures 3, 4, and 5 show the measured spectral response of the 4 × 100 GHz, 8 × 250 GHz, and 12 × 400 GHz AWGs using 28, 40, and 70 waveguides in the

Table 1. Design Overview of Three AWG Sets

Sets (size)	Waveguides	Arm Aperture Width (μm)	Order	Delay Length (μm)	FSR (nm)
4 × 100 GHz	16	3.49	254	146.15	4.3
(1180 × 285 μm^2)	20	2.75	230	116.81	5.3
	24	2.26	169	97.25	6.4
	28	1.91	145	83.44	7.5
8 × 250 GHz	25	2.75	65	37.4	16.8
(540 × 320 μm^2)	30	2.26	54	31.07	20.2
	35	1.91	47	27.05	23.2
	40	1.65	41	23.59	26.6
12 × 400 GHz	40	2.01	26	14.96	42.0
(380 × 330 μm^2)	50	1.57	20	11.51	54.6
	60	1.28	17	9.78	64.2
	70	1.07	15	8.63	72.8

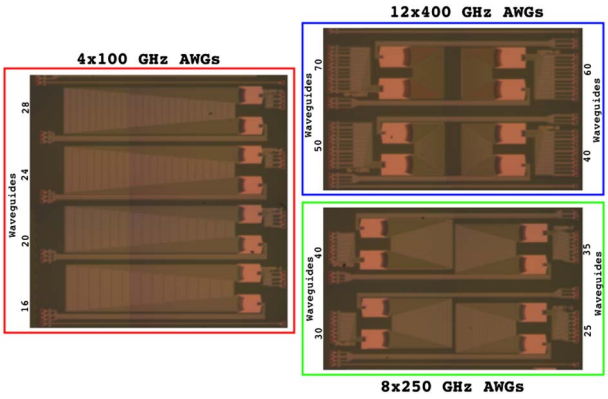

Fig. 2. Optical images of the fabricated AWGs.

array, respectively. The measured FSR for these devices was 6.9, 24.8, and 69.8 nm, respectively. It is immediately obvious that the loss and the crosstalk improve considerably when increasing the AWG channel spacing. As we can see from Figs. 3–5, the shape of the individual AWG channel is sightly asymmetric but similar for all channels of the device. This asymmetry could be due to minor phase variations in the waveguides or due to

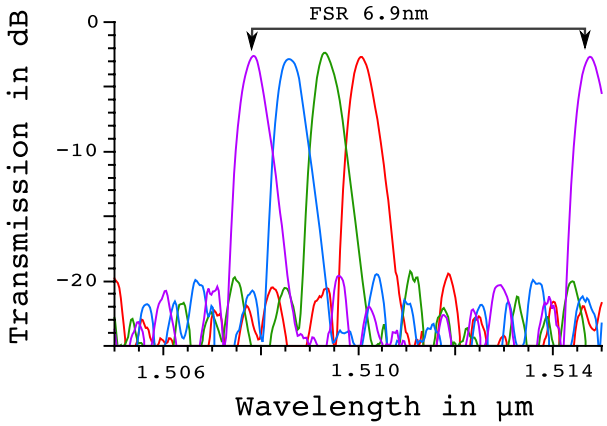

Fig. 3. Experimental spectral response of 4×100 GHz AWG with 28 waveguides used in the array.

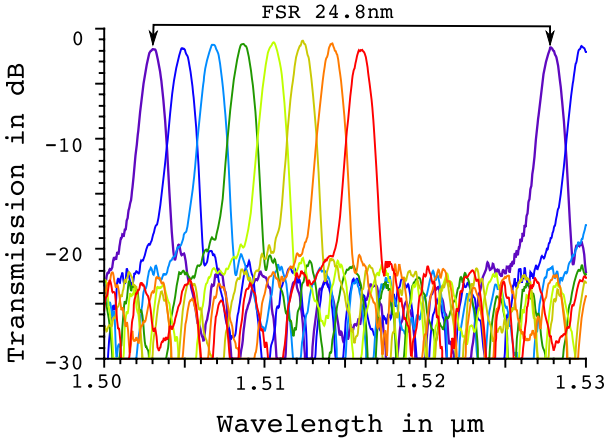

Fig. 4. Experimental spectral response of 8×250 GHz AWG with 40 waveguides used in the array.

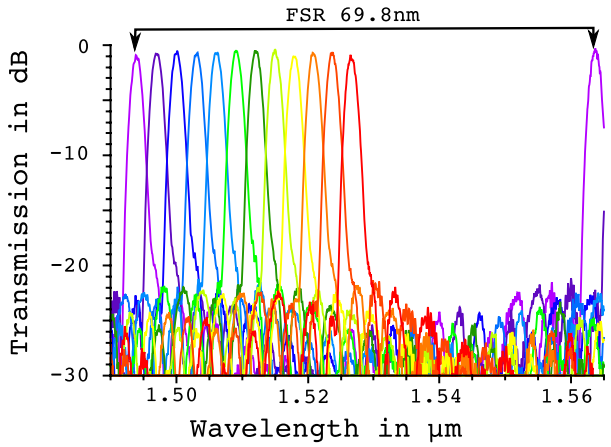

Fig. 5. Experimental spectral response of 12×400 GHz AWG with 70 waveguides used in the array.

the fabrication error in the input aperture of the input star coupler.

Figure 6(a) shows how the insertion loss changes with the variation of the number of waveguides used in the waveguide array. As already mentioned above, the insertion loss improves when going from 100 to 200 GHz and then 400 GHz channel spacing, which is related to the decrease in device size and associated propagation loss. Within one device group the insertion loss improves when increasing the number of waveguides, as predicted in the fourth paragraph. Further improvement is restricted by the critical width of the shallow etched arm apertures to avoid high propagation loss due to an unconfined mode. Figure 6(b) shows the nonuniformity in the insertion loss between the center channel and the outer channel as a function of the number of waveguides in the array. As expected from the reasoning in the previous paragraph, the uniformity improves with increasing FSR.

Due to the high confinement of silicon waveguides, even small geometric variations introduce significant phase errors, resulting in an unwanted crosstalk floor.

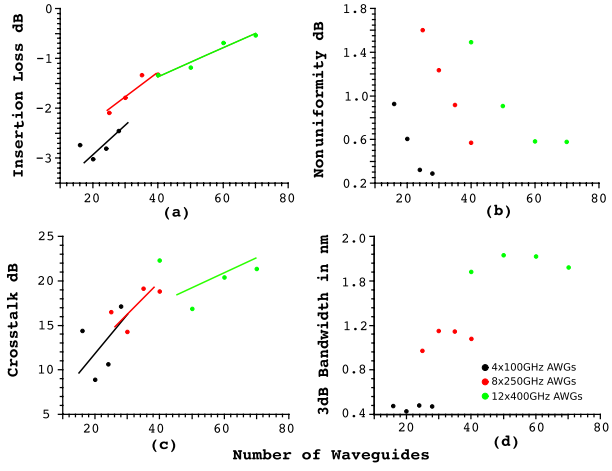

Fig. 6. (a) Insertion loss variation, (b) nonuniformity variation, (c) crosstalk variation, and (d) bandwidth variation with the variation of the number of waveguides used in the array waveguides for 4×100 GHz, 8×250 GHz, and 12×400 GHz AWGs.

Figure 6(c) shows how the crosstalk level changes with the number of waveguides used in the array. The crosstalk level is defined by taking the difference (in decibels) between the crosstalk floor and the center channel loss and as can be seen from Fig. 6(c) improves considerably when increasing the channel spacing. This improvement originates both from an improved center channel loss for the larger channel spacing devices and from an improving crosstalk floor. Within one device group (with fixed channel spacing) the crosstalk level increases when increasing the number of waveguides within the array. In this case the crosstalk floor remains nearly constant between devices but the central channel loss improves significantly. The random sidewall roughness of the waveguide introduces side lobes, which leads to unequal crosstalk variation compared to the center channel loss. It is expected that the overall sidewall roughness of the waveguide will be better for a highly dense array waveguide due to a uniform etch profile during the fabrication process. It is expected that further increasing the number of waveguides results in array waveguides that will not further improve the performance given that in that case the waveguides in the array start to couple, introducing a new crosstalk channel.

Within a group of devices, we expect the bandwidth to be constant as the channel spacing and the star coupler size were fixed (as discussed in the fifth paragraph). But from Fig. 6(d) we can see some small variation in the 3 dB bandwidth. A possible explanation is the random shape changes of a wavelength channel due to variations in the linewidths and local wafer thickness. Alternatively it could be due to a ripple in the transfer characteristics caused by parasitic reflections at the fiber couplers introducing uncertainty on the exact shape of the AWG transfer function.

We demonstrated compact SOI-based AWGs for (de) multiplexing applications with a wide range of wavelength resolutions. The performance of the devices in terms of insertion loss, crosstalk, and nonuniformity improves when we use a larger FSR, and this without increasing the footprint of the device. The best performance is achieved for 4×100 GHz, 8×250 GHz, and 12×400 GHz AWGs with FSRs of 6.9, 24.8, and 69.8 nm, respectively. For these AWGs we measured insertion losses of −2.45, −1.32, and −0.53 dB, respectively. The crosstalk levels of the AWGs are between 17.12 and 21.37 dB, and the nonuniformities vary between 0.286 and 0.567 dB. The footprints of the 100, 250, and 400 GHz AWGs are 1180×285 μm^2, 540×320 μm^2, and 380×330 μm^2, respectively. These results demonstrate that we are able to design and fabricate large FSR SOI-based AWG (de)multiplexers for a wide range of wavelength resolutions with acceptable performance.

The authors acknowledge the multi-project-wafer (MPW) service ePIXfab through which the devices were fabricated. Part of this work was supported by the European Research Council through the ERC Inspectra project.

References

1. K. Takada, M. Abe, M. Shibata, M. Ishii, and K. Okamoto, IEEE Photon. Technol. Lett. **13**, 1182 (2001).
2. C. Dragone, IEEE Photon. Technol. Lett. **3**, 812 (1991).
3. R. Adar, C. Henry, C. Dragone, R. Kistler, and M. Milbrodt, J. Lightwave Technol. **11**, 212 (1993).
4. R. Mestric, H. Bissessur, B. Martin, and A. Pinquier, IEEE Photon. Technol. Lett. **8**, 638 (1996).
5. W. Bogaerts, S. Selvaraja, P. Dumon, J. Brouckaert, K. De Vos, D. Van Thourhout, and R. Baets, IEEE J. Sel. Top. Quantum Electron. **16**, 33 (2010).
6. S. Pathak, M. Vanslembrouck, P. Dumon, D. Van Thourhout, and W. Bogaerts, J. Lightwave Technol. **31**, 87 (2013).
7. J. Zou, X. Jiang, X. Xia, T. Lang, and J.-J. He, J. Lightwave Technol. **31**, 1935 (2013).
8. A. Klekamp and R. Munzner, J. Lightwave Technol. **21**, 1978 (2003).
9. S. Selvaraja, P. Jaenen, W. Bogaerts, D. Van Thourhout, P. Dumon, and R. Baets, J. Lightwave Technol. **27**, 4076 (2009).
10. F. van Laere, G. Roelkens, M. Ayre, J. Schrauwen, D. Taillaert, D. Van Thourhout, T. Krauss, and R. Baets, J. Lightwave Technol. **25**, 151 (2007).